

# Study of QGP signatures with the $\phi \rightarrow K^+ K^-$ signal in Pb-Pb ALICE events

A. Akindinov<sup>1</sup>, A. Alici<sup>2,3</sup>, P. Antonioli<sup>3</sup>, S. Arce<sup>3,4</sup>, M. Basile<sup>2,3</sup>, G. Cara Romeo<sup>3</sup>, M. Chumakov<sup>1</sup>, L. Cifarelli<sup>2,3,4</sup>, F. Cindolo<sup>3</sup>, A. De Caro<sup>5</sup>, D. De Gruttola<sup>5</sup>, S. De Pasquale<sup>5</sup>, A. Di Bartolomeo<sup>5</sup>, M. Fusco Girard<sup>5</sup>, Yu. Grishuk<sup>1</sup>, C. Guarnaccia<sup>5</sup>, M. Guida<sup>5</sup>, D. Hatzifotiadou<sup>3</sup>, D.W. Kim<sup>6</sup>, J.S. Kim<sup>7</sup>, S. Kiselev<sup>1</sup>, G. Laurenti<sup>3</sup>, K. Lee<sup>6</sup>, S.C. Lee<sup>6</sup>, Ye. Lyublev<sup>1</sup>, M.L. Luvisetto<sup>3</sup>, D. Mal'kevich<sup>1</sup>, A. Margotti<sup>3</sup>, A. Martemiyanov<sup>1</sup>, K. Mikhin<sup>1</sup>, R. Nania<sup>3</sup>, F. Noferini<sup>2,3</sup>, A. Pesci<sup>3</sup>, M. Ryabinin<sup>1</sup>, E. Scapparone<sup>3</sup>, G. Scioli<sup>2,3</sup>, A. Selivanov<sup>1</sup>, S. Sellitto<sup>5</sup>, R. Silvestri<sup>5</sup>, A. Smirnitkiy<sup>1</sup>, Y. Sun<sup>7</sup>, G. Valenti<sup>3</sup>, I. Vetlitskiy<sup>1</sup>, K. Voloshin<sup>1</sup>, L. Vorobiev<sup>1</sup>, M.C.S. Williams<sup>3</sup>, D. Yakorev<sup>6</sup>, B. Zagreev<sup>1</sup>, C. Zampolli<sup>2,3</sup>, A. Zichichi<sup>2,3,4</sup>

<sup>1</sup> Institute for Theoretical and Experimental Physics, Moscow, Russia

<sup>2</sup> Dipartimento di Fisica dell'Università, Bologna, Italy

<sup>3</sup> Museo Storico della Fisica e Centro Studi e Ricerche “Enrico Fermi”, Roma, Italy

<sup>4</sup> Dipartimento di Fisica dell'Università and INFN, Salerno, Italy

<sup>5</sup> Department of Physics, Kangnung National University, Kangnung, South Korea

<sup>6</sup> World Laboratory, Lausanne, Switzerland

Received: 28 April 2005 / Revised version: 31 October 2005 /

Published online: 5 January 2006 – © Springer-Verlag / Società Italiana di Fisica 2006

**Abstract.** The  $\phi \rightarrow K^+ K^-$  decay channel in Pb-Pb collisions at LHC is studied through a full simulation of the ALICE detector. The study focuses on possible signatures in this channel of quark-gluon plasma (QGP) formation. On a basis of  $10^6$  collisions at high centrality some proposed QGP signatures are clearly visible both in  $K^+ K^-$  invariant mass and transverse mass distributions. The high significance of this observation appears to reside heavily on the use of the TOF (Time Of Flight) system of ALICE in addition to its central tracking detectors.

## 1 Introduction

High-energy heavy-ion collisions are considered since a long time (see for example [1]) golden events as regards the creation and detection of a quark-gluon plasma (QGP). At SPS a possible evidence for the production of a new state of matter, possibly coinciding with QGP, has been found [2–5]. The results from RHIC heavy-ion experiments appear to confirm the QGP hypothesis, and seem to give evidence of some additional property of the formed plasma [6].

The nature and the characteristics of QGP are in large respects even theoretically unknown. This suggests that a much larger set of measurements is needed to recognize what has been really discovered by the cited experiments and to reconstruct the characteristics of QGP. Presumably only from the convergence of many different experimental signatures can the QGP be fully understood and the QGP interpretation of the data established beyond any doubt.

One of the expected and already detected signatures is tied to the s-quark enhancement accompanying (partial) chiral symmetry restoration. This should raise the strange and multiply strange particle content of the event [7–14].

In this respect the  $\phi$  particle is of particular interest because it is the lightest of the vector mesons with hidden flavour. The production and decay rates of these parti-

cles are strongly influenced by the OZI (Okubo, Zweig, Iizuka) rule, that requires the transitions to be described by connected quark diagrams [15, 16]. A first consequence is that in case of QGP a strong enhancement of the  $\phi$  rate is expected as the system has abundance of s-quarks in the initial state to feed  $\phi$  production. A second consequence is the small cross section of the  $\phi$  for scattering with non strange hadrons. This implies that  $\phi$  particles are only slightly affected by rescatterings with nuclear matter during the expanding phase, rescatterings that could wash out the spectral information of the plasma.

In previous works the capabilities of the future ALICE experiment at LHC [17] in extracting the “normal”  $\phi$  meson signal were discussed, using a full detector Monte Carlo simulation [18, 19]. The aim of this paper is to present the results of a first study, again through full simulation of the apparatus, of the potentialities of ALICE in the detection of QGP signatures in the  $\phi$  signal.

The study of the  $\phi$  in the  $\phi \rightarrow K^+ K^-$  channel has some additional problems with respect to the  $\phi \rightarrow \ell^+ \ell^-$  channel ( $\ell$  stands for leptons). These are mainly related to the fact that kaons are subject to strong interactions, with consequent possible rescatterings with nuclear matter, and that the  $\phi \rightarrow K^+ K^-$  threshold (i.e. twice the kaon mass) and the nominal  $\phi$  mass are close to each other, with phase

space problems in the study of possible modifications of the mass distribution.

On the other hand the  $\phi \rightarrow K^+K^-$  decay has a branching ratio of 0.49 whereas the value for any leptonic decay mode is of the order of  $10^{-4}$ . In addition kaon identification is performed in ALICE with low contamination and high efficiency over a large solid angle within a wide energy range. These circumstances suggest that at least in the initial stage of ALICE data taking, the  $\phi \rightarrow K^+K^-$  should be the most interesting channel for  $\phi$  studies.

The present work investigates the sensitivity of ALICE to QGP signatures connected to the  $\phi$  decay channel into kaons, in the hypothesis that some kind of modifications are present in the  $\phi$  mass distribution and/or in the  $\phi$  momentum spectrum in the plasma phase and that they survive, even if largely distorted, after  $\phi$  and kaon propagation. While performing this, particular attention is paid to the gain in the  $\phi \rightarrow K^+K^-$  analysis coming from the addition to the TPC (Time Projection Chamber [20]) of the TOF (Time Of Flight [21]) system for particle identification (PID). This in view of the fact that the presence of a powerful TOF barrel detector, extending PID at medium/high momenta [21, 22], will be a key of ALICE.

## 2 Physics hints

An enhancement of s-quark production in connection with QGP formation has been predicted since a long time [7, 8]. An enhancement of the  $\phi/\omega$  ratio, as remarked in [23], should point to this effect in a particularly clean way, but also an enhancement in the  $\phi$ /hadron ratio is in general expected.

The s-quark density is readily calculable in case of non-interacting QGP, assuming that the equilibrium level is reached [24, 25]. During the collision however, even if QGP is formed, ordinary nuclear matter is also present and, in any case, QGP evolves to ordinary nuclear matter at freeze-out. In addition an s-quark enhancement can be expected also without QGP formation, as a consequence of pure nuclear effects, so that only the details of the enhancement as a function of nucleon-nucleon center-of-mass energy,  $\sqrt{s_{NN}}$ , could permit to discriminate among QGP and non-QGP scenarios.

It has been suggested that the dependence on  $\sqrt{s_{NN}}$  of the s-quark content in case of QGP formation could be non monotonic [26–28], this being detectable for example in the  $s/\pi$  ratio. Experimental confirmation for this prediction can perhaps be seen [29, 30] from the  $K/\pi$  measurements obtained at AGS/SIS [11], SPS [29] and RHIC [12–14].

Then even though the s-quark enhancement is a very interesting item, there are some ambiguities in the evaluation of the expected amount in case of QGP formation and in the interpretation of the enhancement already detected so far. It is generally believed that this item alone is not (and presumably will not be, in the future) sufficient to constrain to QGP interpretation; other items must be considered in addition.

In the present work we are concerned with signatures of QGP related to the  $\phi$  signal alone. This means that we

will try to estimate the sensitivity with respect to possible changes in some properties of  $\phi$  mesons, for example in their mass distribution, assuming a reasonable scenario for s-quark enhancement at LHC energies.

The  $\phi$  signal in the  $\phi \rightarrow K^+K^-$  decay channel is extracted from the large  $K^+K^-$  combinatorial background. Also this background is influenced by the amount of s-quark enhancement. However if the  $K$  and  $\phi$  yields grow in the same proportion, the  $\phi$  signal significance in first approximation does not change. A key element in the simulations is therefore the  $\phi/K$  ratio.

According to experimental results [12–14, 29, 30], there is no sign of a significant increase in the  $K^+/\pi^+$  ratio going from SPS to RHIC energies, with a kind of plateau already starting at the lowest SPS energies. Different is the situation for the  $K^-/\pi^-$  ratio, for which a rise from SPS to RHIC energies is visible; at the highest energies the two ratios, for positively and negatively charged particles, are almost equal.

As regards the  $\phi$  meson, a monotonic increase in the  $\phi/h^-$  ratio with  $\sqrt{s_{NN}}$  is present [30] ( $h^-$  stands for negative hadrons), starting from few GeV energies [11] and going through SPS [3, 29, 30] to RHIC energies [31, 32]. The  $\phi/K^-$  ratios found at STAR [32–34] and PHENIX [14] appear however to be roughly the same as at top SPS energies [3].

The  $K/\pi$  ratio within the HIJING generator [35] is 0.11 at  $\sqrt{s_{NN}} = 5.5$  TeV, i.e. a bit lower than the RHIC value ( $\sim 0.15$ ) [12–14]. The  $\phi/K^-$  ratio, as measured at RHIC [14, 32–34], is consistent within errors with the HIJING value of 0.16 at 5.5 TeV.

In our simulations we have used the HIJING values at  $\sqrt{s_{NN}} = 5.5$  TeV both for kaon and  $\phi$  multiplicities. As we are referring to LHC energies, this appears to be a rather conservative assumption. In fact the quoted experimental results suggest that above RHIC energies kaon production presumably saturates, whereas there is no indication in this sense for  $\phi$  mesons. As a consequence the  $\phi/K$  ratio at LHC energies is likely to be larger than at RHIC energies.

During heavy-ion collisions at LHC energies,  $\phi$  generation and decay happen in a heterogeneous and variable medium for which two components can be envisaged. One is purely nuclear, consisting of nucleons/hadrons at various number densities and temperatures, but far from  $T_c$ , the critical temperature for the onset of QGP transition; the other one is the foreseen QGP component. The latter may also include a mixed-phase configuration (occurring during plasma expansion) in which some plasma effects still persist. To the former component belong in particular all nucleons/hadrons present after chemical freeze-out<sup>1</sup> is reached. Let us call it in the following the freeze-out component.

To estimate the relative yield of  $\phi$  meson decays from the two components is a quite complicated task. It depends on parameters theoretically largely undetermined and has no hope of experimental assessment at present. In case of a first order phase transition, the estimated duration of the

<sup>1</sup> When, in the evolution of the hadronic system, inelastic collisions cease and particle ratios become fixed.

QGP phase is relatively large ( $\sim 10$  fm/c, comparable with a vacuum lifetime of  $\phi$  mesons of  $\sim 45$  fm/c) and it can be expected that the two yields are comparable [36]. This should hold true even if the phase transition is instead smooth [36], since lattice calculations show that in this case the phase transition is a crossover very close to a first order one [37].

At LHC energies the  $\phi$  mesons if decaying inside the freeze-out component should have their free-space Breit-Wigner mass distribution centred at  $1019.5$  MeV/ $c^2$  with a width of  $4.3$  MeV/ $c^2$ . Modifications of the resonance mass, width and shape can indeed be present in nuclear matter at high density, coming from phase space distortions and dynamical interactions with the medium [38]. They are expected to be observable, but small.

For decays inside the QGP component the foreseen situation is very different. First of all, as a consequence of partial chiral symmetry restoration, the  $\phi$  mass distribution may be at sizeably lower values [39–42]. The exact value of the estimated shift is subject to large uncertainties, depending on the assumptions made in the calculations. The plasma  $\phi$  mass could be 10–20% lower than the nominal mass value, but also very near to it.

Since the kaon mass is expected to change very smoothly with temperature [43], the shifted  $\phi$  mass can also be well below the  $K^+K^-$  decay threshold in the plasma. This implies that in principle the width of the resonance should decrease in the plasma. However the width is also influenced by additional effects related to the presence of a medium. These could result from an attractive kaon potential favouring  $\phi$  decays [44] (negligible when the  $\phi$  mass is well below the two-kaon mass) or from  $\phi$  interactions with surrounding hadrons, such as  $\pi$ ,  $K$ ,  $\rho$  and  $\phi$  itself, enabling  $\phi$  decay modes otherwise not present in free-space [43, 45] and changing the  $\phi$  spectral function. As a net result an increase of the width up to  $\sim 10$  MeV [43] can fairly be expected. Further few MeV are expected to come through the interactions with partons in the plasma [46]. The calculated width depends on the effective interaction model chosen to describe the plasma. Some choices can give even larger widths, of the order of a few tens of MeV, as in the case of [47].

On top of this, as we are studying  $\phi$  decays in the  $\phi \rightarrow K^+K^-$  channel, we must consider the effects on the observed width of kaon collisions with light mesons, both for the freeze-out and QGP components. In-medium kaon collisions change the kaon spectral function (off-shell kaon final states) and, as a consequence, the  $\phi$  decay rate. In addition, in-medium (QGP or freeze-out) rescatterings of on-shell kaons should have an influence on the measured width. In principle these rescatterings can even completely wash out the signal. In the present work we assume that a sizeable fraction of  $\phi \rightarrow K^+K^-$  decays occurring in the QGP component is “useful” to produce a signal with an additional width, due to off-shell kaon effects coupled with kaon rescattering effects, comparable with the original  $\phi$  width. Also in the case of decays in the freeze-out component, a width larger than the normal one has been used as a way to describe in-medium effects.

According to theoretical expectations [36] as well as to experimental hints [14, 31, 33], the transverse momentum (or transverse mass) distribution of  $\phi$  mesons generated inside the freeze-out component at LHC should be harder than the distribution found at RHIC, that is with an inverse slope (i.e. temperature) parameter  $T$  larger than the RHIC measured value:  $T = 379 \pm 50 \pm 45$  MeV [31], or  $T = 363 \pm 8$  (stat.) MeV (at 0–5% centrality, with similar values for other centralities) [33], or  $T = 366 \pm 11 \pm 18$  MeV (minimum bias) [14].

On the contrary a much softer distribution is expected for  $\phi$  particles generated inside the QGP component, with  $T \simeq T_c$  (independently of the initial temperature [36]) and typical expected values for  $T_c$  in the range 160–180 MeV. Due to the small probability of rescattering of the  $\phi$  mesons after chemical freeze-out [23], the  $\phi$  particles generated in the plasma should retain their energy distribution in the plasma even when they subsequently decay in the freeze-out component. All this suggests that transverse mass<sup>2</sup> ( $m_t$ ) distributions are another powerful tool, in addition to invariant mass ( $m_{\text{inv}}$ ) distributions, to extract evidence for QGP formation from the data and, in case, to derive  $T_c$  from slope measurements [36].

The expected line-shapes of  $K^+K^-$  invariant and transverse mass distributions emerging from the described scenario are then as follows.

The  $m_{\text{inv}}$  distribution can have two peaks, one localized at the normal (free space)  $\phi$  mass value and the other at lower values. The normal peak should correspond to  $\phi$  particles either produced and decaying in the freeze-out component or produced in the QGP component but decaying afterwards in the freeze-out one. The lower mass peak should be formed by  $\phi$  mesons produced and decaying in the plasma.

A “bridge” between the two peaks can be expected, reflecting the possible mixed-phase evolution from plasma to chemical freeze-out.

The lower mass peak can also be missing; of course this may occur when the  $\phi$  mass in the plasma is lower than the two-kaon threshold. On the other hand, the QGP peak can also be so near to the normal freeze-out peak to be practically undistinguishable. However, even in this case, a signature of QGP formation could be searched for in the  $m_t$  distribution as we will see later on. A double component could/should in fact be present, one (QGP) mostly present at low  $m_t$  values and the other one (freeze-out) surely dominant at large values.

### 3 Simulation strategy

Orders of  $10^5$ – $10^6$  events turned out to be needed to simulate a significant signal for the present analysis. Direct full generation, tracking and reconstruction of such a huge number of events, corresponding to very high multiplicity final states from central Pb-Pb interactions, was estimated a rather severe task and simulations have been instead organized in two steps, as follows.

<sup>2</sup>  $m_t = (m_{\text{inv}}^2 + p_t^2)^{1/2}$ .

In the first step, some hundred central<sup>3</sup> HIJING [35] events, with  $\sqrt{s_{NN}} = 5.5$  TeV, were generated, tracked, digitized and reconstructed, making use of detailed simulations of all ALICE detectors (see [18, 19]). In these simulations a magnetic field of 0.4 T was used.

From these simulations the relevant parameters for the subsequent second step were extracted, as a function of transverse momentum ( $p_t$ ), namely the momentum resolution (in modulus and direction) and, both for the TPC and the TOF, the PID efficiencies [18, 19]. The momentum is measured by the TPC and the resolutions used are detailed in [18, 19] (for  $p_t$  in the range 0.2–9.0 GeV/c, the relative  $p_t$  resolution varies between 1% and 2% and the angular resolutions go from 5.0 to 0.3 mrad for both polar and azimuthal angles); the TPC PID capability relies on  $dE/dx$  measurements.

In the second step  $10^6$  events were generated, each event containing an average of 850 charged kaons. This is the number expected from HIJING Pb-Pb central events at  $\sqrt{s_{NN}} = 5.5$  TeV in the pseudorapidity ( $\eta$ ) interval  $[-1, 1]$ .

The kaons are generated with independent random choices of rapidity ( $y$ ) and  $p_t$ . The  $y$  distribution is a gaussian with  $\sigma = 4$  [18, 19]. The kaon  $p_t$  distribution is obtained through the  $m_t$ -scaling method starting from the corresponding distribution for pions; for the latter, for  $p_t < 0.5$  GeV/c, an  $m_t$ -scaling spectrum has been assumed with  $T = 160$  MeV and, for  $p_t > 0.5$  GeV/c, the power law parametrization reported in [48] has been chosen. This gives a kaon  $m_t$  distribution with an inverse slope parameter varying with  $m_t$ ; its fitted value being 309 MeV for  $(m_t - m)$  in the range 0–1 GeV/c<sup>2</sup>, and 390 MeV in the range 1–2 GeV/c<sup>2</sup>, where  $m$  is the nominal kaon mass. Both  $y$  and  $m_t$  distributions are the same as used in [18, 19].

In each event an average number of 85 additional charged kaons (that is 10% more) were generated according to the same distributions to take into account in a simple but conservative manner [21] contamination effects mainly coming from pions. An average number of 35  $\phi \rightarrow K^+K^-$  decays per event was also added, with both kaons inside the indicated  $\eta$  range. Given the chosen amount of generated kaons, this number corresponds to the already quoted  $\phi/K^-$  ratio of HIJING.

The  $\phi$  particles are similarly generated through independent random choices of  $y$  and  $p_t$  and they are allowed to decay isotropically in the center-of-mass frame. Their  $y$  distribution is the same as reported above for kaons, as in [18, 19]. Their  $p_t$  distribution, differently from [18, 19], was not obtained through the  $m_t$ -scaling method used for kaons. It required instead a dedicated approach, according to the purpose of the present work where we have tried to study the sensitivity to QGP signatures when the input  $\phi$  mass and  $p_t$  distributions are actually affected by QGP formation. To this aim  $\phi$  mass distributions different from the PYTHIA [49] one have been chosen and particular  $m_t$  distributions, for  $\phi$  mesons generated in both the QGP and the freeze-out components, have been used.

<sup>3</sup> The impact parameter range used in HIJING is 0–3 fm. The resulting average charged particle density at mid-rapidity is  $\langle dN_{ch}/dy \rangle \sim 6500$ .

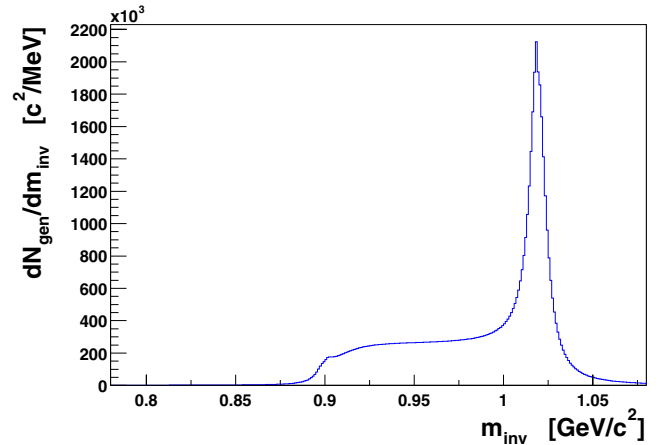


**Fig. 1.** All-decay  $\phi$  mass distribution for case A (see text); the  $\phi$  mass inside the plasma is assumed to be below the two-kaon threshold; only a small fraction of  $\phi$  particles are allowed to decay inside the plasma fireball; a sizeable fraction is assumed to decay in a mixed environment corresponding to the evolution phase from plasma to dense nuclear matter, which gives rise to the so-called “bridge” region

For each event all kaons were finally processed according to momentum resolutions and PID efficiencies extracted from the first step simulation [18, 19].

Concerning the generation of the  $\phi$  invariant mass spectrum, two very different situations may appear: one (call it case A) in which the  $\phi$  mass inside the plasma (referred to as QGP  $\phi$  mass in the following) is below the two-kaon mass threshold and another one (case B) in which it is above.

For case A, the results turn out to be quite insensitive to the exact value of the QGP  $\phi$  mass as well as to the relative importance between the pure QGP part and the freeze-out part of the  $\phi$  mass distribution. What is crucial instead is the contribution assumed for the “bridge” region, corresponding to the evolution from QGP to chemical freeze-out.

In Fig. 1 an example of generated  $\phi$  mass distribution representative of case A is reported. Here all  $\phi$  decay modes are included (with the  $\phi$  produced in the  $y$  interval  $[-1, 1]$ ) and  $m_{inv}$  is the invariant mass of any decay products. Two (QGP and freeze-out) Breit-Wigner peaks, each with an enlarged width  $\Gamma = 10$  MeV/c<sup>2</sup>, are assumed. The freeze-out peak is centred at the nominal  $\phi$  mass value ( $m_0$ ). The additional “bridge” region is taken as a uniform (flat) distribution extending from one peak maximum to the other. Normalization is such that the number of  $\phi \rightarrow K^+K^-$  decays (strictly speaking, the number of useful  $\phi$  decays, in the sense explained in Sect. 2) is obtained through multiplication by a factor  $\Psi(m)/\Psi(m_0)$ , where  $\Psi(m)$  and  $\Psi(m_0)$  are the 2-body  $K^+K^-$  phase space factors, respectively, at  $\phi$  masses  $m$  and  $m_0$ . This gives zero  $\phi \rightarrow K^+K^-$  actual decays below the two-kaon threshold. The peak around the chosen QGP  $\phi$  mass (0.9 GeV/c<sup>2</sup>) is, in this example, depressed. The population of  $\phi$  decays within the “bridge” region is assumed instead equal to that of the freeze-out peak, i.e. the peak above the  $KK$  threshold, at the nominal  $\phi$  mass.

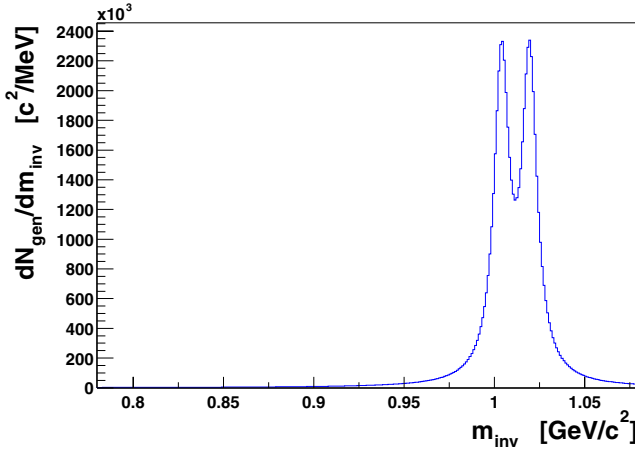


**Fig. 2.** All-decay  $\phi$  mass distribution for case *B* (see text); the  $\phi$  mass inside the plasma is assumed to be above the two-kaon threshold

For case *B*, the results both in the  $K^+K^-$  invariant mass line-shape and in the  $K^+K^-$  transverse mass spectrum depend on the exact location of the chosen QGP  $\phi$  mass.

In Fig. 2 (analogous to Fig. 1) an example of  $\phi$  mass distribution generated for case *B* is reported. In this example, the QGP  $\phi$  mass peak is at  $m = 1004 \text{ MeV}/c^2$ , which is approximately half way between the  $KK$  threshold and the nominal  $\phi$  mass. Here the two Breit-Wigner peaks are assumed to be equally populated and the additional “bridge” region strongly depressed.

Turning now to the corresponding  $m_t$  spectra, these are described by fixed inverse slope parameters. For  $\phi$  particles generated in the freeze-out component, the value  $T_0 = 480 \text{ MeV}$  (with a spectrum close to that in [18, 19]) has been chosen. This value is higher than the measured RHIC values [14, 31, 33] quoted in Sect. 2, thus allowing to take into account the effects of a larger initial temperature at LHC energies. The critical temperature for the transition to QGP has been assumed to be  $T_c = 180 \text{ MeV}$ , hence this value was chosen for  $\phi$  mesons generated in the plasma [36].

For each  $\phi$  mass distribution used in the present exercise (Fig. 1 or 2), the corresponding  $m_t$  distribution is the sum of only two components. The first, with inverse slope  $T_0$ , corresponds to  $\phi$  meson decays belonging to the freeze-out Breit-Wigner peak; the second, with inverse slope  $T_c$ , to all the other  $\phi$  decays belonging to the QGP peak and the additional “bridge” (if any). As said in Sect. 2, the freeze-out Breit-Wigner peak should in principle collect all  $\phi$  decays occurring in the freeze-out, no matter where the  $\phi$  mesons are actually produced (although most of them would likely be produced in the freeze-out). Therefore assuming for the whole freeze-out peak a unique temperature  $T_0$  corresponds to neglect, as a first approximation, the cases in which the  $\phi$  is generated in the plasma (or in the “bridge”) and decays in the freeze-out.

## 4 Results and discussion

Figure 3 shows the inclusive  $m_{\text{inv}}$  distribution for all identified  $K^+K^-$  pairs relative to the  $10^6$  simulated events ob-

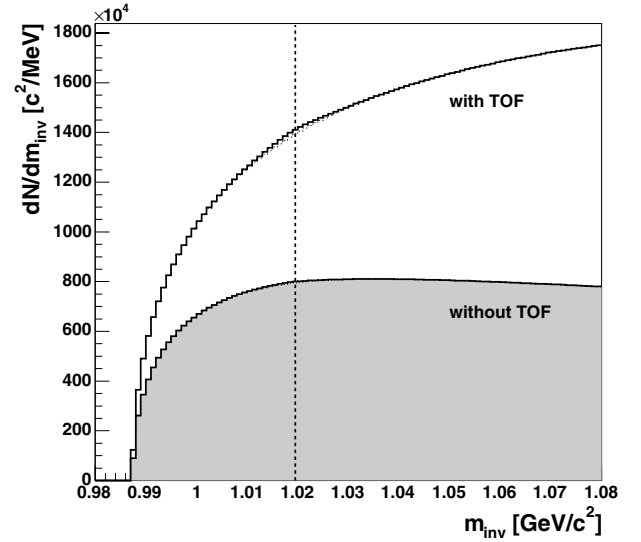


**Fig. 3.** Invariant mass distribution for all opposite-sign identified kaon pairs in  $10^6$  events. The normalized (see text) background distribution relative to equal-sign identified kaon pairs is superimposed. The results with/without TOF are compared.

tained as described in Sect. 3, using as input the single-peak  $\phi$  mass spectrum of Fig. 1 (case *A*). The ALICE detector effects are taken into account and two configurations are compared: one in which the TOF system is not present in the detection and PID chain (“without TOF”), the other in which the TOF system is also considered (“with TOF”). The difference in the  $K^+K^-$  pair population for the two cases is evident; there is roughly a ratio 1.8 in the regions just below and above the nominal  $\phi$  mass. This difference is obviously determined by the enlargement, thanks to the TOF, of the momentum region where kaons can be identified.

A significant  $\phi$  signal can be extracted after background subtraction. For the background we have used analogous  $m_{\text{inv}}$  distributions corresponding to all equal-sign identified kaon pairs<sup>4</sup>. The result is shown in Fig. 4. This figure actually represents what can happen when the QGP  $\phi$  mass is below the  $KK$  threshold.

In Fig. 4, again a comparison is made between the results with and without the TOF system. The ratio between the two peak heights is about 3.3, that is significantly larger than the above 1.8 ratio between the two background levels (with and without TOF, in Fig. 3); the  $\phi$  signal significance is correspondingly enhanced by a factor  $\sim 3.3/\sqrt{1.8} \sim 2.5$ . This shows that the larger momentum acceptance for PID, only achievable when the TOF is included in the analysis, reflects itself in a larger signal/background ratio, due to the different spectral properties of background kaons with respect to kaons coming from  $\phi$  meson decays.

The fit to the data (with TOF) reported in Fig. 4 is a Breit-Wigner weighted with the appropriate phase space factor. The fit parameters,  $m_0 = 1018.6 \text{ MeV}/c^2$  and  $\Gamma =$

<sup>4</sup> The like-sign ( $K^+K^+$ ,  $K^-K^-$ ) background is normalized to the  $K^+K^-$  spectrum in the mass regions below and above the  $\phi$  peak.

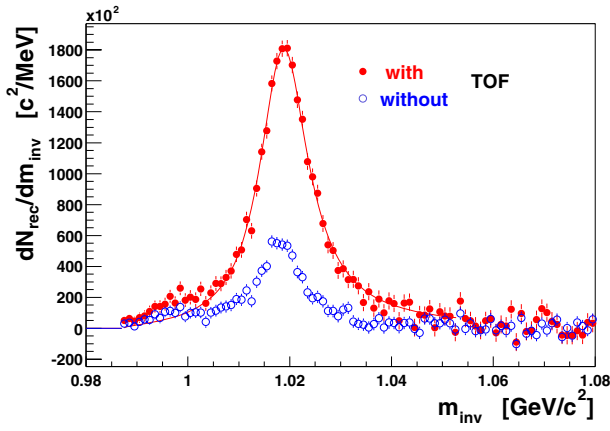


**Fig. 4.** Extracted signal after background subtraction. The assumed  $\phi$  mass input spectrum is that of Fig. 1 (when the  $\phi$  mass inside the plasma is below the two-kaon threshold). The results with/without TOF are compared

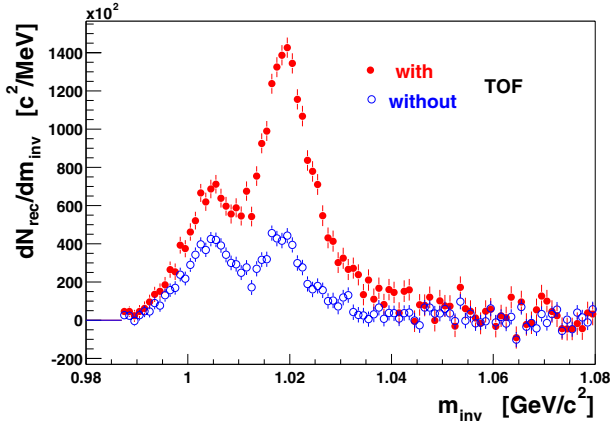


**Fig. 5.** Same as Fig. 4 but relative to the  $\phi$  mass input spectrum of Fig. 2 (when the  $\phi$  mass inside the plasma is above the two-kaon threshold)

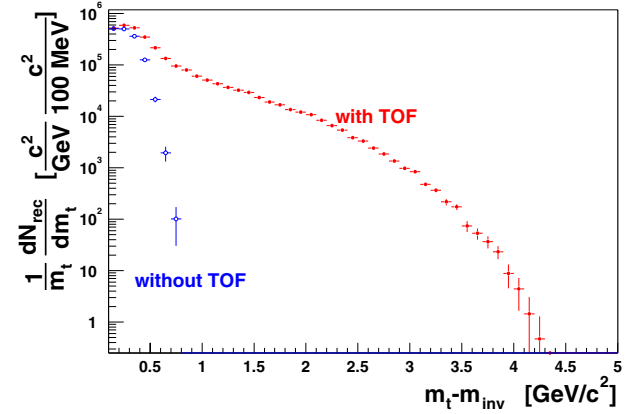
$11.5 \text{ MeV}/c^2$ , are in accordance with the input parameters used in this exercise and with the excellent mass resolution of the detector [18,19]. A small excess of events with respect to the fit is visible, on the left side of the peak; this excess comes from  $\phi \rightarrow K^+K^-$  decays in the “bridge” region defined in Sects. 2 and 3.

Figure 5 shows the  $K^+K^-$  invariant mass distribution for the signal after background subtraction, when the  $\phi$  mass inside the plasma is above the  $KK$  threshold (case *B* of Sect. 3); this figure corresponds now to the  $\phi$  mass input spectrum of Fig. 2. Here a double peak structure appears. One can notice that, with TOF, the QGP  $\phi$  mass peak is depressed with respect to the freeze-out peak, despite the fact that the two peaks are equal in the input spectrum of Fig. 2, while, without TOF, the two peaks remain balanced. This is a consequence of the different phase space factors for the two peaks, combined with the different PID efficiencies vs. momentum for the TPC and TOF detectors.

When the peaks are too near, they become practically undistinguishable and other ways should be searched in order to disentangle a QGP contribution. Table 1 reports the  $\phi$  signal significance (within  $\pm\Gamma/2$  from the mean, with

**Table 1.**  $\phi$  signal significance for case *B* (see text) in  $10^6$  events; the  $\phi$  mass inside the plasma is assumed to be above the two-kaon threshold and the all-decay  $\phi$  mass input spectrum to contain equally populated QGP and freeze-out peaks.

| QGP $\phi$ mass<br>(GeV/ $c^2$ ) | significance<br>without TOF |            | significance<br>with TOF |            |
|----------------------------------|-----------------------------|------------|--------------------------|------------|
|                                  | QGP                         | freeze-out | QGP                      | freeze-out |
| 0.99                             | 32.8                        | 41.3       | 39.2                     | 112.2      |
| 1.                               | 41.9                        | 37.4       | 53.0                     | 98.7       |
| 1.01                             | 48.7                        | 43.3       | 74.0                     | 101.5      |
| 1.02 (nominal)                   | 67.7                        |            | 128.1                    |            |



**Fig. 6.**  $(m_t - m_{inv})$  distribution of the signal after background subtraction. The assumed  $\phi$  mass input spectrum is that of Fig. 1, corresponding to a plasma  $\phi$  mass below the two-kaon threshold. The results with and without TOF are compared

$\Gamma = 10 \text{ MeV}/c^2$ ) for both peaks and for various choices of the QGP  $\phi$  mass. The results are given with and without TOF<sup>5</sup>.

One can see from this table that the signal significance on a basis of  $10^6$  collision events is actually very high. In principle, with a statistics of only some 20,000 events, a significant  $\phi$  signal should already appear. The point is however that important handles to disentangle a QGP signal are the details of the invariant mass line-shape and, as we will see next, of the transverse mass distribution. In view of this a superabundant significance of the signal is mandatory.

As said, a promising signature of QGP formation could show up in  $m_t$  distributions. Figure 6 reports the  $K^+K^-$  ( $m_t - m_{inv}$ ) distributions relative to the signal in Fig. 4

<sup>5</sup> It can be noticed that the with/without TOF significance ratios in this table – from top to bottom – increase from 1.2 to 1.5 for the QGP peak and decrease from 2.7 to 1.9 for the freeze-out peak. Again this is a consequence of the different temperatures assumed for the two (QGP and freeze-out) components and of the different performances vs.  $p_t$  of the two (TPC and TOF) detectors. In particular this explains why when the QGP and freeze-out peaks are superimposed (last table row) the significance gain due to the TOF is lower than for the single freeze-out peak of Fig. 4.



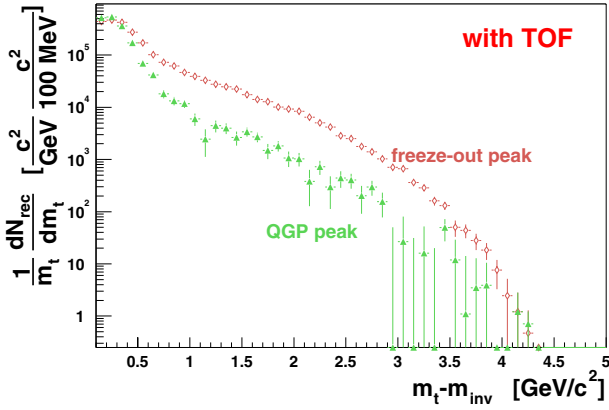


**Fig. 7.**  $(m_t - m_{\text{inv}})$  distribution of the signal after background subtraction, in two different regions of invariant mass (see text and Fig. 5): one around the vacuum value (freeze-out peak) and the other one around the plasma value (QGP peak). The assumed  $\phi$  mass input spectrum is that of Fig. 2, corresponding to a plasma  $\phi$  mass above the two-kaon threshold

(referring to the input spectrum of Fig. 1) for the cases with and without TOF. The background is subtracted using the same procedure as for Fig. 4. The distributions are not corrected for detector  $K^+K^-$  transverse mass acceptance<sup>6</sup>, just to show how large is the improvement obtained by adding the TOF. In particular, the region with  $(m_t - m_{\text{inv}}) > 0.8 \text{ GeV}/c^2$  cannot be explored without the inclusion of this detector [19].

In Fig. 6 one can see that the  $m_t$  acceptance in the configuration without TOF falls off very rapidly for  $(m_t - m_{\text{inv}})$  below  $1 \text{ GeV}/c^2$ . In these circumstances uncertainties in  $m_t$  acceptance would heavily interfere with genuine  $m_t$  spectra and make the QGP discrimination a very difficult task, contrary to what happens if the PID capability of the TOF is enabled.

Figure 7 allows to determine the  $m_t$  region relevant for QGP discrimination. The figure refers to the input spectrum of Fig. 2 and shows the  $K^+K^-$   $(m_t - m_{\text{inv}})$  distributions (with TOF) for the signal in Fig. 5, after background subtraction, in two  $m_{\text{inv}}$  regions: one corresponding to the QGP and the other to the freeze-out Breit-Wigner peak. Each region in Fig. 5 is selected within  $\pm\Gamma/2$  around the corresponding  $m_{\text{inv}}$  peak value. Here again the distributions are not corrected for detector  $K^+K^-$  transverse mass acceptance. The difference in slope of the two distributions is clearly evident up to  $(m_t - m_{\text{inv}}) \simeq 1.5 \text{ GeV}/c^2$ , with a softer spectrum relative to the QGP peak. Above this value the shapes of the distributions become quite similar. This indicates that the contamination from freeze-out decays within the QGP peak range grows with  $(m_t - m_{\text{inv}})$  and becomes nearly 100% above that value.

The input spectrum of Fig. 2 has been chosen as an example of a particularly clean situation, to show the principle of the discrimination between QGP effects and freeze-out

effects. Nevertheless, using the present  $10^6$  event data sample and taking advantage of the TOF PID, it can be shown that a similar discrimination in  $m_t$  spectra can be achieved for every location of the QGP peak above the  $KK$  threshold (assuming for definiteness equal heights for the two peaks in the all-decay  $m_{\text{inv}}$  distribution). When the two peaks are very near or exactly superimposed, the two  $m_t$  spectra refer to the same  $m_{\text{inv}}$  regions around the nominal  $\phi$  mass value; in this case QGP effects are still visible as a change in the slope of the spectrum, becoming harder above  $(m_t - m_{\text{inv}}) \simeq 0.5 \text{ GeV}/c^2$ .

Such an  $m_t$  discrimination thanks to the TOF is in principle still viable when the QGP  $\phi$  mass is below the  $KK$  threshold, as in the situation of Figs. 1 and 4, even though with smaller statistical significance. The two  $m_{\text{inv}}$  regions to be compared in this case are the freeze-out peak and a narrow region just above the  $KK$  threshold.

As also ordinary nuclear matter can give some shift in the resonance mass as well as a distortion in its shape [38], the presence of anomalies in invariant mass distributions of the kind described in Figs. 4 and 5 could fail to be a compelling indication of QGP formation. Then the use of the additional  $m_t$  information turns out crucial to obtain such an indication, whichever the invariant mass line-shape is.

In the results shown above the signal has been extracted, as we have seen, through a procedure of uncorrelated background subtraction. Background is however expected to be uncorrelated only at first approximation. As there is no knowledge of particles decaying to  $K^+K^-$  with mass near the nominal  $\phi$  mass, the most interesting sources of correlated background potentially relevant for the present analysis are particles with  $\pi p$ ,  $\pi K$  or  $\pi\pi$  decays where one or both decay products are misidentified as kaons.

The probability that the PID procedure misidentifies a pion or a proton as a kaon does not exceed the few % level [18, 19]. This rules out any significant contribution from  $\pi\pi$  or  $\pi p$  decays of abundantly produced nearby particles such as  $K_S^0$  or  $\Lambda^0$  (moreover, for the former, kinematics pushes this contribution mainly above the  $m_{\text{inv}}$  region of interest). Hence in practice only  $\pi K$  decays can have a relevance. For this kind of decays the best candidate is  $K^{0*}$ . But again, in addition to a  $\sim 10^{-2}$  reduction factor from PID efficiency, almost all contamination decays from this meson are shifted to  $m_{\text{inv}}$  values larger than the nominal  $\phi$  mass due to kinematics. The assumption of uncorrelated background appears then fairly safe.

A last comment regards final-state kaon interactions. All the results obtained reside on the assumption that a non negligible number of  $\phi$  decays have the kaons coming out from the plasma with momenta resembling their initial momenta (the so called useful  $\phi$  decays, see Sect. 2). To change this number, i.e. to change the relative importance of the QGP and freeze-out components in the all-decay input spectra (Figs. 1 and 2), implies to change the significance of QGP discrimination. With a reduced number of useful decays this discrimination can of course become impossible.

On the other side it seems quite difficult to reproduce the described signatures of QGP formation through reinteractions of kaons (or of pions and protons misidentified as kaons) coming from decays of resonances other

<sup>6</sup> This to allow the cleanest possible comparison (i.e. without introducing additional biases deriving from the fact that the correction for  $m_t$  acceptance maintains a dependence from the input spectra assumed for  $\phi$  production).

than the  $\phi$ . Re-interactions will presumably spread kaon (and other particle) momenta and distort their spectra, but it seems unlikely that they would be able to mimic combined signatures of the kind described herein in both the invariant mass and transverse mass distributions. From this one can infer that if such signatures are observed they would strongly point to an origin not easily reducible to final-state interaction effects, and contribute to compel to a QGP scenario.

## 5 Conclusions

In this work the sensitivity of ALICE to QGP signatures in Pb-Pb collisions has been investigated through full detector simulation by studying the  $\phi \rightarrow K^+K^-$  decay channel.

The impact of QGP formation on two quantities, the mass and the transverse momentum of  $\phi$  mesons produced inside the plasma, has been considered.

On a basis of  $10^6$  central events, a discrimination of QGP effects has been shown to be possible for various choices of  $\phi$  mass inside the plasma, even below the  $KK$  threshold. This can be achieved by looking at secondary peaks or distortions of the invariant mass distribution of the extracted signal in the region below the nominal  $\phi$  mass and at the spectral properties (transverse mass distribution) of this signal.

The combined study of both the  $m_{\text{inv}}$  and the  $m_t$  distributions of  $\phi$  mesons has been identified as a powerful tool of investigation.

The significance of the results depends on various theoretical unknowns such as the QGP  $\phi$  mass value, the duration of the QGP phase, the evolution mechanism of the system from plasma to chemical freeze-out, the particle ratios and spectra, among others.

Experimentally this significance would strongly benefit from the TOF system for particle identification. The overall  $\phi$  signal significance is actually found to be enhanced by a factor 2–3 thanks to the TOF; moreover, this gain in significance strongly increases with  $m_t$  while, in the configuration without the TOF, no sensitivity is present when  $(m_t - m_{\text{inv}})$  is above  $0.8 \text{ GeV}/c^2$ . This means that the effectiveness in QGP discrimination in terms of  $m_t$  appears to depend crucially on the presence of the TOF PID capability.

## References

1. M. Jacob, Nucl. Phys. A **418**, 7c (1984)
2. U. Heinz, M. Jacob, nucl-th/0002042 (2000) and references therein
3. M. Gaździcki (NA49 Collab.), J. Phys. G **30**, S701 (2004)
4. A. Marin (CERES Collab.), in proc. of XXXVIIth Rencontres de Moriond: QCD and High Energy Hadronic Interactions, Les Arcs, France (2002), hep-ex/0205105
5. G.E. Bruno (NA57 Collab.), J. Phys. G **30**, S717 (2004)
6. M. Gyulassy, NATO Advanced Study Institute: Structure and Dynamics of Elementary Matter, Kemer, Turkey (2003), nucl-th/0403032 (2004) and references therein
7. J. Rafelski, B. Müller, Phys. Rev. Lett. **48**, 1066 (1982)
8. J. Rafelski, Nucl. Phys. A **418**, 215c (1984)
9. B.B. Back et al. (E917 Collab.), Phys. Rev. C **69**, 054901 (2003)
10. S.V. Afanasiev et al. (NA49 Collab.), Phys. Lett. B **491**, 59 (2000)
11. L. Ahle et al. (E802 Collab.), Phys. Rev. C **57**, 466 (1998); Phys. Rev. C **58**, 3523 (1998); Phys. Rev. C **60**, 044904 (1999); L. Ahle et al. (E866 and E917 Collaborations), Phys. Lett. B **476**, 1 (2000); Phys. Lett. B **490**, 53 (2000); J. Barrette et al. (E877 Collab.), Phys. Rev. C **62**, 024901 (2000); D. Pelte et al. (FOPI Collab.), Z. Phys. A **357**, 215 (1997)
12. J. Adams et al. (STAR Collab.), (2003) Phys. Rev. Lett. **92**, 112301 (2004)
13. K. Adcox et al. (PHENIX Collab.), Phys. Rev. Lett. **88**, 242301 (2002)
14. S.S. Adler et al. (PHENIX Collab.), nucl-ex/0410012 (2004)
15. S. Okubo, Phys. Rev. D **16**, 2336 (1977)
16. H. Lipkin, Phys. Lett. B **60**, 371 (1976)
17. N. Ahmad et al. (ALICE Collab.), Technical Proposal, CERN/LHCC 95-71, LHCC/P3, 15 December 1995
18. A. De Caro et al., Internal Note ALICE-INT-2003-067 and references therein
19. A. De Caro, The ALICE TOF (Time-Of-Flight): a powerful detector for relevant observables in nucleus-nucleus collisions at LHC, Ph.D. Thesis, Bologna University (2004), <http://alice.sa.infn.it/PhDthesisAdeCaro.ps.gz>
20. N. Ahmad et al. (ALICE Collab.), Time Projection Chamber, Technical Design Report, CERN/LHCC 2000-001, ALICE TDR 7, 7 January 2000
21. N. Ahmad et al. (ALICE Collab.), Time of Flight System, Technical Design Report, CERN-LHCC 2000-12, ALICE TDR 8, 16 February 2000; P. Cortese et al. (ALICE Collab.), Time of Flight System, Technical Design Report, Addendum, CERN-LHCC 2002-016, Addendum to ALICE TDR 8, 24 April 2002
22. A. Akindinov et al. (ALICE TOF Collab.), Eur. Phys. J. **C32S1**, 165 (2004)
23. A. Shor, Phys. Rev. Lett. **54**, 1122 (1985)
24. S. Danos, J. Rafelski, Phys. Rev. D **27**, 671 (1983)
25. G. Domokos, J. Goldman, Phys. Rev. D **23**, 203 (1981)
26. M. Gaździcki, D. Röhrich, Z. Phys. C **65**, 215 (1995); C **71**, 55 (1996) and references therein
27. M. Gaździcki, Z. Phys. C **66**, 659 (1995)
28. M. Gaździcki, M.I. Gorenstein, Acta Phys. Polon. B **30**, 2705 (1999) and references therein
29. S.V. Afanasiev et al. (NA49 Collab.), Phys. Rev. C **66**, 054902 (2002)
30. A. Mischke (NA49 Collab.), Int. Europhys. Conf. on High Energy Phys., Aachen, Germany (2003), Eur. Phys. J. C **33**, S621 (2004)
31. C. Adler et al. (STAR Collab.), Phys. Rev. C **65**, 041901 (2002)
32. T.S. Ullrich, Nucl. Phys. A **715**, 399c (2003) and references therein
33. J. Adams et al. (STAR Collab.), (2004) nucl-ex/0406003
34. C. Markert (STAR Collab.), J. Phys. G **30**, S1313 (2004)
35. X.-N. Wang et al., Phys. Rev. D **44**, 3501 (1991); Phys. Rev. Lett. **68**, 1480 (1992)
36. M. Asakawa, C.M. Ko, Phys. Lett. B **322**, 33 (1994); Phys. Rev. C **50**, 3064 (1994)



37. F.R. Brown et al., Phys. Rev. Lett. **65**, 2491 (1990);  
F. Karsch, E. Laermann, A. Peikert, Phys. Lett. B **478**,  
447 (2000)
38. P. Fachini, J. Phys. G **30**, S735 (2004)
39. R.D. Pisarski, Phys. Lett. B **110**, 155 (1982)
40. T. Hatsuda, T. Kunihiro, Phys. Rev. Lett. **55**, 158 (1985);  
T. Hatsuda, Nucl. Phys. A **544**, 27 (1992)
41. M. Asakawa, C.M. Ko, Phys. Rev. C **48**, 526 (1993); Nucl.  
Phys. A **560**, 399 (1993)
42. S. Gao et al., Phys. Rev. C **49**, 40 (1994); H.-C. Jean et  
al., Phys. Rev. C **49**, 1981 (1994); H. Shiomi, T. Hatsuda,  
Nucl. Phys. A **590**, 545c (1995)
43. C.M. Ko, D. Seibert, Phys. Rev. C **49**, 2198 (1994)
44. D. Lissauer, E. Shuryak, Phys. Lett. B **253**, 15 (1991);  
E. Shuryak, V. Thorsson, Nucl. Phys. A **536**, 739 (1992)
45. P.Z. Bi, J. Rafelski, Phys. Lett. B **262**, 485 (1991)
46. D. Seibert, C.M. Ko, Phys. Rev. C **50**, 559 (1994)
47. L. Holt, K. Haglin, J. Phys. G **31**, S245 (2005)
48. F. Abe et al. (CDF Collab.), Phys. Rev. Lett. **61**, 1819  
(1988)
49. H.U. Bengtsson, T. Sjöstrand, Comput. Phys. Commun.  
**46**, 43 (1987)